

Mechanism of the high transition temperature for the 1111-type iron-based superconductors $R\text{FeAsO}$ ($R = \text{rare earth}$): Synergistic effects of local structures and $4f$ electrons

Lifang Zhang,^{1,2} Junling Meng,¹ Xiaojuan Liu,^{1,*} Fen Yao,^{1,3} Jian Meng,¹ and Hongjie Zhang¹¹State Key Laboratory of Rare Earth Resources Utilization, Changchun Institute of Applied Chemistry, Chinese Academy of Sciences, Changchun, Jilin 130022, China²University of Science and Technology of China, Hefei, Anhui 230026, China³University of Chinese Academy of Sciences, Beijing, 10049, China

(Received 19 January 2017; revised manuscript received 21 June 2017; published 14 July 2017)

Among the iron-based superconductors, the 1111-type Fe-As-based superconductors $\text{REFeAsO}_{1-x}\text{F}_x$ ($\text{RE} = \text{rare earth}$) exhibit high transition temperatures (T_c) above 40 K. We perform first-principles calculations based on density functional theory with the consideration of both electronic correlations and spin-orbit couplings on rare earths and Fe ions to study the underlying mechanism as the microscopic structural distortions in REFeAsO tuned by both lanthanide contraction and external strain. The electronic structures evolve similarly in both cases. It is found that there exist an optimal structural regime that will not only initialize but also optimize the orbital fluctuations due to the competing Fe-As and Fe-Fe crystal fields. We also find that the key structural features in REFeAsO , such as As-Fe-As bond angle, intrinsically induce the modification of the Fermi surface and dynamic spin fluctuation. These results suggest that the superconductivity is mediated by antiferromagnetic spin fluctuations. Simultaneously, we show that the rare-earth $4f$ electrons play important roles on the high transition temperature whose behavior might be analogous to that of the heavy-fermion superconductors. The superconductivity of these 1111-type iron-based superconductors with high- T_c is considered to originate from the synergistic effects of local structures and $4f$ electrons.

DOI: [10.1103/PhysRevB.96.045114](https://doi.org/10.1103/PhysRevB.96.045114)

I. INTRODUCTION

Since the discovery of superconductivity in $\text{LaFeAsO}_{1-x}\text{F}_x$ with critical temperature T_c 26 K in early 2008 [1], various types of iron pnictides containing square lattices of Fe^{2+} have been investigated [2–4]. To explain the emergence of superconductivity near the antiferromagnetic (AFM) phase, a spin fluctuation model resulting from Fermi surface nesting between hole and electron pockets was proposed based on density-functional theory (DFT) calculation [5,6]. Superconductivity emerges when the tetragonal-orthorhombic structural transition and paraantiferromagnetic phase transition are suppressed by carrier doping or pressure application. Also, it has been found that some important aspects of the electronic structures, such as Fermi surfaces [7–9] and antiferromagnetic coupling [10,11], of iron oxypnictides depend very sensitively on small changes in interatomic distances and bond angles within the iron-pnictogen subunit. Particularly, by replacing the La atoms with other rare-earth elements and modulating the structural parameters, new superconductors were discovered and T_c was quickly enhanced in $\text{SmFeAsO}_{1-x}\text{F}_x$, $\text{CeFeAsO}_{1-x}\text{F}_x$, $\text{PrFeAsO}_{1-x}\text{F}_x$, and $\text{NdFeAsO}_{1-x}\text{F}_x$ to above 50 K [12–15]. Experimental facts indicate that the Fe-As-based superconductors have a much higher T_c than other Fe-based superconductors and, furthermore, only the 1111-type Fe-As-based superconductors exhibit a high- T_c above 40 K [16]. However, the underlying mechanism of this high- T_c has not yet been clarified until now [17].

So far, the dominating ways to induce superconductivity are carrier-doping by aliovalent substitution [11,18], chemical pressure by lanthanide contraction [14,15], and external

pressure [19]. However, except for pressure application, for both carrier doping and chemical pressure, two effects are simultaneously identified. Such as the role of the chemical substitutions, carrier doping, and a steric one, “chemical pressure” caused by the difference in size between for example Ba^{2+} and K^+ or O^{2-} and F^- , should be considered at the same time [20]. While for chemical pressure by lanthanide contraction, the contribution from the $4f$ electrons should be simultaneously taken into account since it is well known that $4f$ electrons not only hybridize with anions but also are involved into the magnetic coupling at a certain low temperature, especially at the temperature where superconductivity emerges. Experimentally, it is impossible to separate these factors in the exploration of the superconductive mechanism. Nevertheless, under this circumstance, the recent developments of the first-principles calculations based on the DFT [21] have promoted a breakthrough on studying the electronic state in the strongly correlated electron systems, which is benefit for us to have an insight into the intrinsic mechanism of superconductivity more clearly. The superconducting behavior is closely related to the pairing mechanism [17,22,23]. Identifying the details of their electronic structures, which may be closely correlated to superconductivity, is crucially important to understand the underlying mechanism. Such microscopic studies will give us useful hints for the advancement of other superconductors with higher T_c .

However, no investigations have been carried out with sufficient details to resolve the changes in crystal and electronic structure of the superconducting REFeAsO compounds. Here, we first take lanthanide contraction as fine structural controller, which makes the quasicontinuous structural tuning realized and provides the platform to investigate the structural and electronic structures evolution within these superconductors. Particularly, we notice that external strain, which is also widely

*lxjuan@ciac.ac.cn

used to tune physical properties of functional materials, has not yet been probed until now in these superconductors. Thus, external strain is employed as another way to tune the structural features, whose effect will be intimately compared with that of lanthanide contraction. Relating the observed differences to relevant differences in the electronic structures may provide important clues into the nature and the origin of magnetism and superconductivity in these materials. Subsequently, we discuss that the second possible intrinsic driving force for superconductivity is mediated by the strongly correlated f electrons, whose behavior might be similar to that of the heavy-fermion superconductors [24–27].

II. CALCULATIONAL DETAILS

In this paper, we used the Vienna *ab initio* simulation package (VASP) [28,29] to relax the lattice structures of REOAsFe in $P4/nmm$ space group with the experimental lattice parameters $a = 4.0355 \text{ \AA}$, $c = 8.7393 \text{ \AA}$ [1,11] for REFeAsO (RE = La, Ce, Pr, Nd, Pm, Sm, Gd, Tb, Dy, Ho, Er, Tm, and Lu). Based on both non-spin-polarized and spin-polarized calculations on different levels, including local density approximation (LDA), LDA + U , generalized gradient approximation (GGA), GGA + U , and compared with available experimental determinations, it was found that non-spin-polarized GGA method [30,31] was sufficient to obtain the crystal structures, and it was believed that the lanthanide contraction and external strain effects could be properly simulated on this level. All lattice parameters and atomic positions were fully relaxed until the Hellmann–Feynman force was less than 0.05 eV \AA^{-1} . Our calculations of electronic properties were done by using the GGA of Perdew, Burke, and Ernzerhof (PBE) functional [30,32] within the full-potential linearized augmented plane wave (LAPW) method [33] as implemented in the WIEN2K package [34]. Here, the muffin-tin radii R_{MT} for La, Fe, As, and O were initialized to be 2.34, 2.20, 2.10, and 2.02 a.u., respectively. To ensure convergence, the LAPW basis set was defined by the cutoff $R_{\text{MT}}^{\text{min}} K_{\text{max}} = 9$ (the minimum of R_{MT} and the maximum plane-wave cutoff parameter K_{max}). $19 \times 19 \times 8$ k -point grid was used to perform the Brillouin zone integration [35] in the self-consistent calculations with charge convergence until 10^{-4} eV. For this strongly correlated system with transition metal Fe and lanthanide ions, we took the Coulomb repulsion into account via applied Hubbard interaction (U) [21,36] on the Fe-3d ($U_{\text{Fe}} = 0.5 \text{ eV}$) and RE-4f ($U_{\text{RE}} = 5.0 \text{ eV}$), and simultaneously considered the spin-orbit coupling (SOC) [37] on Fe and RE atoms in the electronic structure simulations. Fe-Fe AFM configurations in the Fe-As layers were considered since it had been observed not only in the experiments [11,38] but also in the theoretical predictions [7,39].

III. RESULTS AND DISCUSSIONS

A. Structural distortions under lanthanide contraction and external strain

All REFeAsO compounds are supposed to crystallize in a tetragonal layered structure [1,11,13]. The unit cell consists of two formula subunits with eight atoms limits to the symmetry of $P4/nmm$, in which Fe-As layers and RE-O layers are

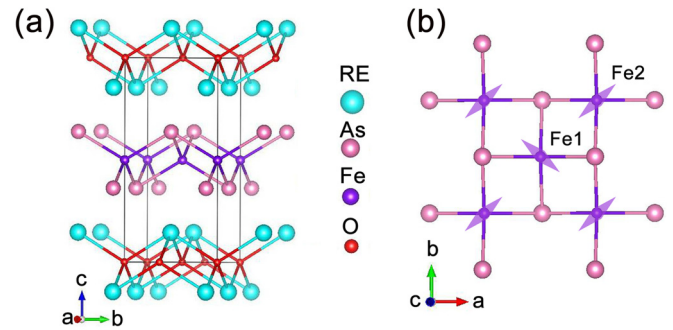


FIG. 1. (a) Crystal structure of REFeAsO with $P4/nmm$ space group. (b) The checkerboard collinear antiferromagnetic order schematic of the Fe-As layer, the pointers represent the magnetic orientation of each Fe-ion and Fe1, Fe2 are labeled.

arranged alternating along the c axis as shown in Fig. 1(a). The Fe-As layers consist of a square lattice sheet of Fe coordinated by As-ions above and below the plane to form face-sharing FeAs_4 tetrahedra. The previous results suggest that the most effective way to increase T_c in iron-based superconductors is to gain the ideal Fe-As tetrahedron since the geometry of the Fe-As tetrahedron might be correlated with the density of states near the Fermi energy [11,20]. Hence, the layers of iron tetrahedrally coordinated by arsenic are crucial structural ingredients. Within these tetrahedra, the key parameters are Fe-As-Fe bond angles ($\alpha_{\text{Fe-As-Fe}}$) and Fe-Fe, Fe-As distances, while Fe-RE distances are also considered since this distance is closely correlated with the interaction dimension within these compounds. Furthermore, another important structural parameter, which is the out-of-plane angles, named as $\beta_{\text{As-Fe1-Fe2}}$, is worthy of attention.

Figure 2 summarizes the impact of lanthanide contraction (or chemical pressure) and external strain on the crystal structures, which all of the relevant structural parameters are obtained from structural relaxation by non-spin-polarized GGA method. Lanthanide contraction gradually suppresses both the a - and c -axis lattice constants [see Fig. 2(a)], in contrast, external strain suppresses only the a - b plane while leaving the c -axis gradually increase [see Fig. 2(f)]. Thus, under this circumstance, our detailed analysis of the relevant parameters, including the distances of Fe-As, Fe-Fe, and Fe-RE and $\alpha_{\text{Fe-As-Fe}}$ and $\beta_{\text{As-Fe1-Fe2}}$, reveals that lanthanide contraction (chemical pressure) systematically reduces the Fe-As, Fe-Fe, and Fe-RE distances and $\alpha_{\text{Fe-As-Fe}}$ [see in Figs. 2(b)–2(e)]. In some more details, the Fe-As distance decreases from 2.327 \AA to 2.320 \AA when RE changes from La to Lu. The Fe-Fe distance is 2.854 \AA when RE is La while it is only 2.720 \AA for Lu, which is short enough for direct Fe-Fe interaction to become important. A decrease in the Fe-Fe distance is known to increase T_c in FeAs superconductors [11]. While the Fe-RE distance is changed from 3.659 \AA to 3.537 \AA from La to Lu, and this parameter has been found to be closely related to the interaction dimension. For the most key parameter $\alpha_{\text{Fe-As-Fe}}$, it is considered that the structural perfection of the Fe-As tetrahedron is important for the high- T_c superconductivity in these Fe pnictides and reaches its maximum value for the ideal Fe-As tetrahedral angle [40,41]. These results suggest that the main effect of lanthanide contraction is to modulate

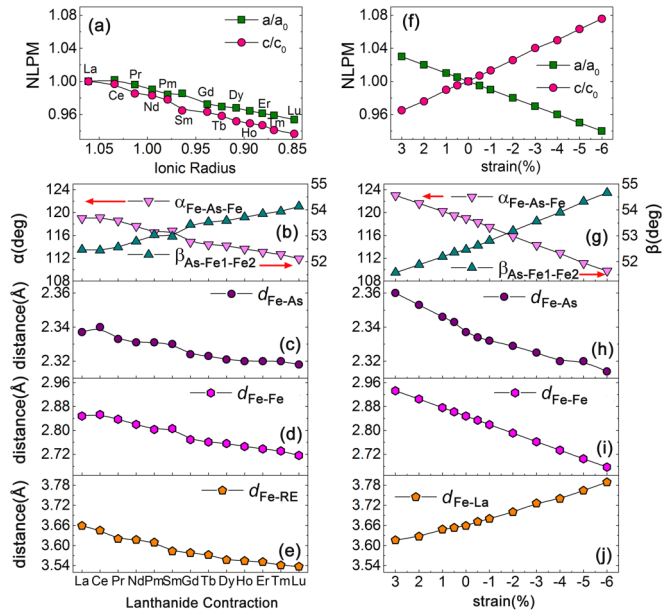


FIG. 2. (a) Lanthanide contraction dependence of the normalized lattice parameter (NLP) variation ($a_0 = 4.02752$, $c_0 = 8.60606$ Å). (b) Varying pattern of the bond angle ($\alpha_{(Fe-As-Fe)}$, $\beta_{(As-Fe1-Fe2)}$) with the lanthanide substitution. (c)–(e) The interatomic distances ($d_{(Fe-As)}$, $d_{(Fe-RE)}$ and $d_{(Fe-Fe)}$) changing tendencies along with the lanthanide contraction. (f)–(j) Structural parameters evolution with the external strain: (f) normalized LPMs, (g) bond angles, (h)–(j) interatomic distances.

the structural distortions and the distance between RE-O and Fe-As blocks. It is anticipated that there should exist an optimal structure, which maximizes the orbital degeneracy around the Fermi level, which is balanced by the competition of Fe-As-Fe and Fe-Fe crystal fields.

Experimentally, external pressure has been applied on the iron-based compounds to induce the superconductivity [20,42]. Herein, we carried out a series of structural strain in the parent compound LaFeAsO. The comparison of the structural evolution of external strain with those of lanthanide contraction suggests that the relevant structural parameters evolve similarly except that Fe-RE distance inversely increases with the increase of external strain [see Figs. 2(f)–2(j)].

B. Insight into the evolution of electronic structures

LaFeAsO is a parent compound of iron-based superconductor [7]. Taking lanthanide contraction as structural controller, we probe the detailed evolution of the electronic structures along the delicate structural changes, aiming at the understanding of the correlation between microstructural distortions and superconductivity. Moreover, taking the external strain as another structural controller, the comparison of electronic structures changing tendency between these two different structural controllers will benefit for us to discuss the physical origin of the superconductivity more deeply. To separate the two factors of $4f$ electrons and structural changes by lanthanide contraction on the electronic structures, we have carried out all the REFeAsO ($RE = Ce \sim Lu$) electronic structures by the calculation of LaFeAsO based on their

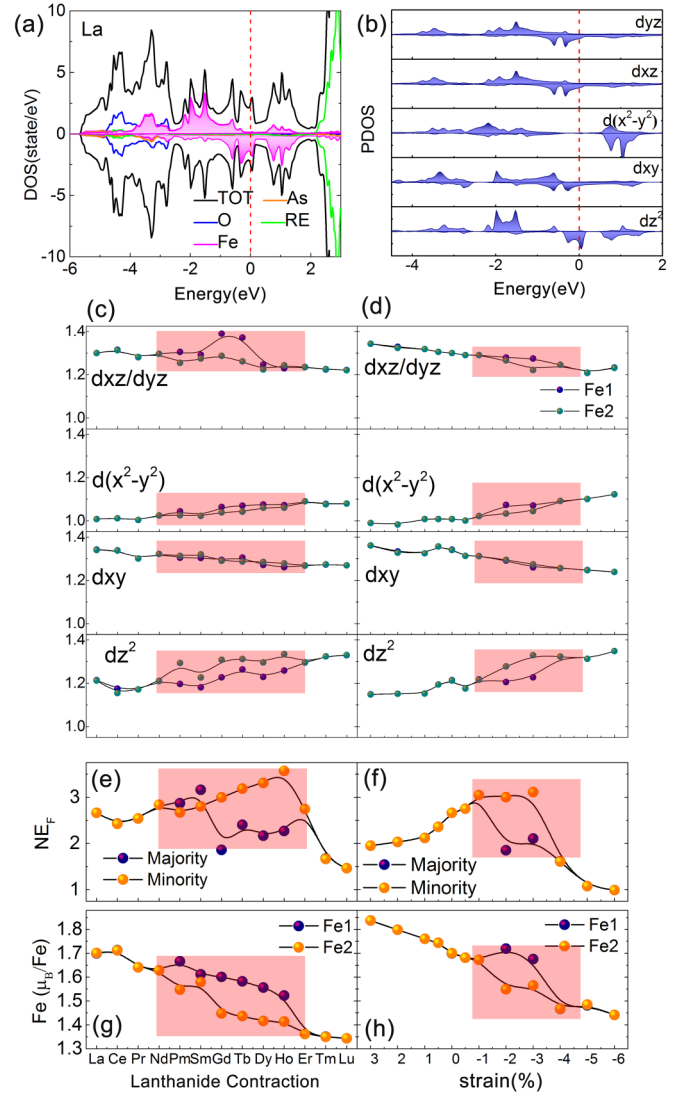


FIG. 3. (a) The density of states (DOS) of parent compound LaFeAsO, the pink shadow highlights Fe1 total orbital distribution. (b) The partial DOS of Fe1 3d electrons within LaFeAsO. (c, d) Each iron 3d electrons (n_v) occupancy on the normal state as functions of the lanthanide contraction and the external strain. (e, f) The evolution of $N(E_F)$ with the lanthanide contraction and external strain, in which $N(E_F)$ means the DOS on the Fermi level; the light red area indicates the spin fluctuation region. (g, h) Dependencies of Fe1 and Fe2 magnetic moment on the lanthanide contraction and external strain, AFM fluctuation area is highlighted with the light red.

respective relaxed structures. Within these stoichiometric parent compounds, it has been widely believed that the itinerant iron 3d electrons form an antiferromagnetic (AFM) order state. Taking LaFeAsO as an example, we first obtain the general character of the electronic structures, including the atomic orbital-projected density of states, electron-hole analysis by band structures. Then, we probe these electronic parameters changing tendency in detail with the finely controlled structures by both lanthanide contraction and external strain.

The atomic-projected density of states (DOS) and band structures are shown in Figs. 3(a) and 4(a), respectively, which are achieved by GGA + U + SOC method. Our calculated

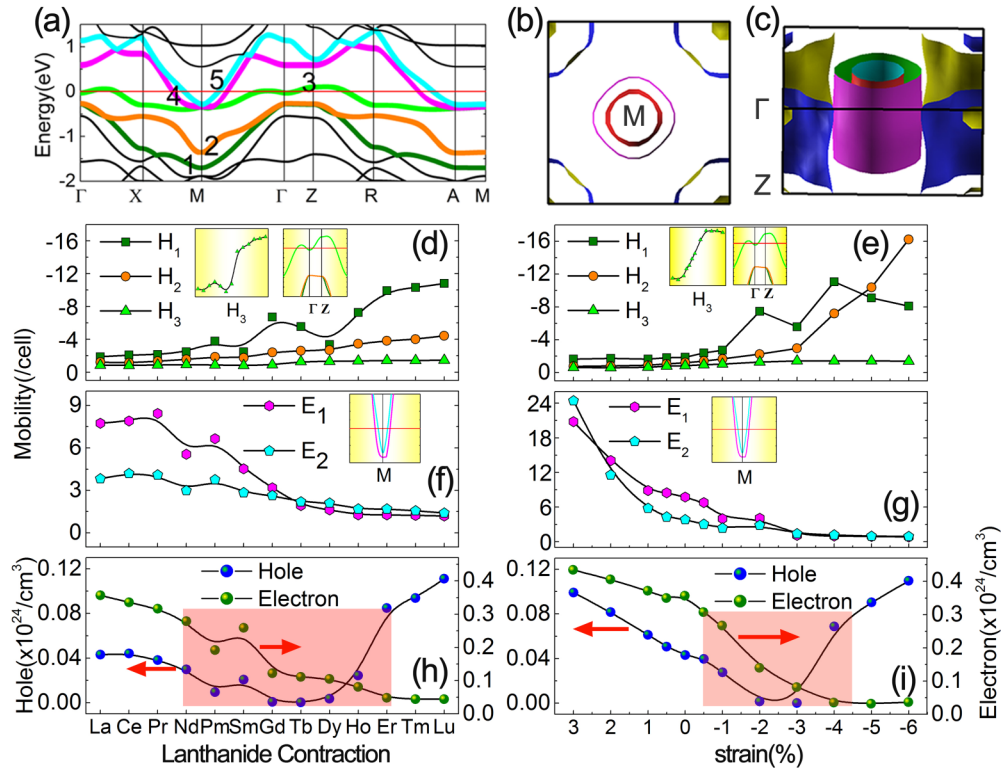


FIG. 4. (a) The electronic band structure of LaFeAsO, in which iron $3d$ contributed bands are labeled by numbers. (b, c) The 2D and 3D Fermi-surface of LaFeAsO, high symmetric point M, Γ and Z in the Brillouin zone are marked in the schematic. The figures are divided into two columns, the left column graphs show the effect of lanthanide contraction and the right ones demonstrate the one of external strain. (d, e) The mobile hole at Γ -Z path change with structural distortion, the upper insert is the partial band structure (the color of each band is consistent with H_1 , H_2 , and H_3), and the bottom one is the magnified H_3 mobility. (f, g) The electron-mobility variation at M high symmetric point, the insert is the partial band structure in M point. (h, i) The transition ranges of hole-pocket and electron-pocket at Fermi surface, blue spheres indicate the volume of hole-pocket and green ones represent the electrons.

results are similar to those in Refs. [8,43,44]. From Fig. 3(a), we can see that LaFeAsO is a semimetal with the Fe $3d$ states accounting for the bands between -2.5 and 2.0 eV and La derived states occurring at higher energy. At the lower energy, from -2.5 eV to -5.5 eV, these states come from O- $2p$ and As- $3p$ states. Fe- $3d$ states would like to split into a lower lying e_g manifold and higher lying t_{2g} states in the Fe-As tetrahedral crystal field. However, this crystal field competes with the direct Fe-Fe interaction, resulting in a more complicated band structure, as the structural analysis above. Subsequently, some important aspects of the electronic structures of the iron oxypnictides depend very sensitively on small changes in interatomic distances and bond angles within the iron-pnictogen subunit. And it is believed that subtle tuning of the microstructures would directly influence this competition. Then, the microelectronic structures related to the orbital fluctuations should be closely correlated and strongly relevant to the superconductivity. In the following, we comprehensively analyze the change of the orbital degree of freedom along with the lanthanide contraction and external strain.

The orbital-projected density of states for Fe ions are shown in Fig. 3(b), in which the five $3d$ states of Fe split into dxz/dyz , dx^2-y^2 , dxy , and dz^2 under the competing crystal fields within P4/nmm space group. We have an exploration on the change of density of states for these orbitals along the lanthanide contraction, and the results are shown in Fig. 3(c). Usually, the

states distribution for the two antiferromagnetically coupled Fe ions [here labeled as Fe1 and Fe2 in Fig. 1(b)] should be the same; however, it is found that there exist some difference between Fe1 and Fe2 when the structural controller hand pointing from Nd to Er. This result demonstrates that within these itinerant AFM systems there exists an optimal competing balance between Fe-Fe and Fe-As-Fe crystal fields, which could maximize the orbital fluctuations. Figures 3(e) and 3(g) shows that these orbital fluctuation should be directly correlated to the charge and then to the spin fluctuations. From the orbital-projected DOS results, it can be inferred that these fluctuations mainly come from the z -direction correlated orbitals dxz/dyz and dz^2 . For the external strain structural controller, plotted in Figs. 3(d), 3(f), and 3(h), there also exist the structural variation range and orbital fluctuation, but being comparatively small and weak than those tuned by lanthanide contraction. These results provide us a microscopic guidance to design novel high-NdFeAsO_{0.85} iron-based superconductors. Experimentally, it was found that the La-based compounds displayed a dome-shaped curve with the pressure dependence of T_c while both the superconducting NdFeAsO_{0.85} and SmFeAsO_{0.85} (have the highest- T_c of around 55 K) showed negative pressure coefficients with T_c decreasing linearly from its initial value with external pressure [16]. Combing these facts and present calculated results, it is considered that within LaFeAsO the structural parameters does not reach the optimal

point while within SmFeAsO and NdFeAsO the structural parameters have reached the optimal balance, and this is why La-based compounds display a dome-shaped curve while Nd/Sm-based compounds show negative pressure coefficients. These results are in complete consistence with our calculated results which will be shown in the following. This indicates that either by lanthanide contraction or by external strain, there is an optimal structural range, within which the electron density of states remarkably degenerate around the Fermi level, demonstrating that orbital degeneracy around the Fermi surface is a key microscopic factor to induce superconductivity with high temperature. It seems that this system shares the importance of multiorbital degrees of freedom. And in this multiorbital system, there exists the orbital degree of freedom, moreover, the orbital fluctuation observed in our calculations could be maximized by the control of microscopic structural parameters.

The Fermi-surface topology, which is crucially important for unconventional superconductivity, can be experimentally clarified by the quantum oscillation and angle-resolved photoemission spectroscopy measurements and so on [45,46]. Theoretically, the Fermi surface could be obtained from our GGA + U + SOC calculation. Figures 4(a), 4(b), and 4(c) show that the Fermi surface is made up of five sheets derived from the five bands crossing the Fermi energy marked by numbers 1, 2, 3, 4, and 5. Among these five sheet, the two sheets originating from two electron bands marked by 4 (purple) and 5 (cyan) are forming two cylinderlike shapes centred around M-A, and the other three from three hole bands marked by 1 (green), 2 (orange), and 3 (reseda green) are forming two cylinderlike shapes centered around Γ -Z and one pocket around Z, respectively. The calculated results are in complete consistence with others [7,8]. Again we explore quantitatively the electron and hole number change along the lanthanide contraction and further compared with those of external strain. The volumes enclosed by these Fermi sheets are analyzed and shown in Figs. 4(d) and 4(e), Figs. 4(f) and 4(g) for the effects of lanthanide contraction and external strain, respectively. In general, the volumes enclosed by 1 (H_1), 2 (H_2), and 3 (H_2) (the hole number) are increasing with lanthanide contraction and external strain while those enclosed by 4 (E_1) and 5 (E_2) (the electron number) are decreasing. Specially, H_1 , E_1 , and E_2 seem to be more sensitive to the change of structural parameters. The changes of the total number of electrons and holes are shown in Figs. 4(h) and 4(i). For both structural controllers, with the larger crystal parameters, the number of electrons is more than that of holes, while crossing a critical point (Ho for lanthanide contraction and -3% for external strain at present calculation level), the number of holes becomes more than that of electrons. Within these 1111-type iron-based superconductors, it has been found that the electron pairing state is an s_{\pm} -wave state with loop-shaped nodes on the Fermi surface [27], our calculated results demonstrate that there seemingly exist a balance between the number of electrons and holes which might contribute to the superconductivity.

C. $4f$ electrons contribution to the superconductivity

For these 1111-type iron-based superconductors REFeAsO (RE are La, Ce, Pr, Nd, Pm, Sm, Gd, Tb, Dy, Ho, Er, Tm, and

Lu), most of the stoichiometric parent compounds exhibit the same in-plane Fe AFM (here we proposed checkboard AFM state), while the c -axis nearest-neighbor spins are different. For examples, for CeFeAsO [11] and PrFeAsO [47,48], c -axis spins are parallel while for both LaFeAsO [40] and NdFeAsO [38], they are antiparallel. Moreover, the magnetic moments of Fe vary at a large range from only $0.25 \mu_B/\text{Fe}$ for NdFeAsO to $0.94 \mu_B/\text{Fe}$ for CeFeAsO. Obviously, different rare earth elements not only influence the magnetic structures but also affect the absolute values of magnetic moments of Fe, implicating that rare earths play an important role for the superconductivity. It has been well-known that magnetic fluctuation is crucially important to make mobile electrons bound strongly within these 1111-type superconductors [8]. However, it has been not clear how the different observed Fe AFM structures/moments for different rare-earth oxypnictides could be explained by their differences in electronic structures since most of the calculations have been carried out for LaFeAsO.

This AFM order has been explained from both the itinerant [18,49] and the localized-electron [50] point of view. This magnetic order couples intimately with a structural distortion. These facts imply also that the Coulomb repulsion, especially a magnetic fluctuation, is crucially important to make mobile electrons bound strongly. Here, assuming that Fe magnetic orderings for all the REFeAsO compounds have the same spin structure as that of LaFeAsO and that the observed AFM order in different rare-earth oxypnictides indeed arises from a spin-density-wave (SDW) instability in a nested Fermi surface [5,7,18], we explore the effect of $4f$ electrons to the superconductivity from two points of view. One is the magnetic coupling between RE and Fe, to this end, the direction of the magnetic moments for the RE are switched while keeping the Fe ions antiferromagnetically coupled. The other is the $4f$ electrons contribution to the Fermi surface. Apparently, these two factors are both closely related to the superconductivity and the transition temperatures.

As mentioned above, REFeAsO-series of compounds possess rare earths RE, which carry local magnetic moments [13] and therefore are different from the non-magnetic La in LaFeAsO. We need to determine whether there exist strong coupling between the Fe and RE moments within these materials. Taking REFeAsO (RE = Pr, Nd, Sm, Gd, Tb) as examples, we switched the direction of magnetic moments of rare earth as shown in Figs. 5(a) and 5(b), then the charge density and magnetic moments on the antiferromagnetically coupled Fe ions (denoted as Fe1 and Fe2) were analyzed. Inspection of Figs. 5(c), 5(d) and Figs. 5(e), 5(f) immediately reveals that the magnitude of the magnetic moments for Fe1 and Fe2 are different and closely related to the direction of the rare earth magnetic moments. Moreover, it is indeed observed that their absolute values of magnetic moments and their variations with the rare-earth directions are different for different rare earth elements. This suggests that there exist strong coupling between RE and Fe. Recently, it has been found that the highly tunable magnetic moment direction and propagation vector observed in CrAs opened up different avenues of research into the interplay between noncollinear helimagnetism and unconventional superconductivity [51]. Here, the presence of the strongly spin-orbit coupling in the

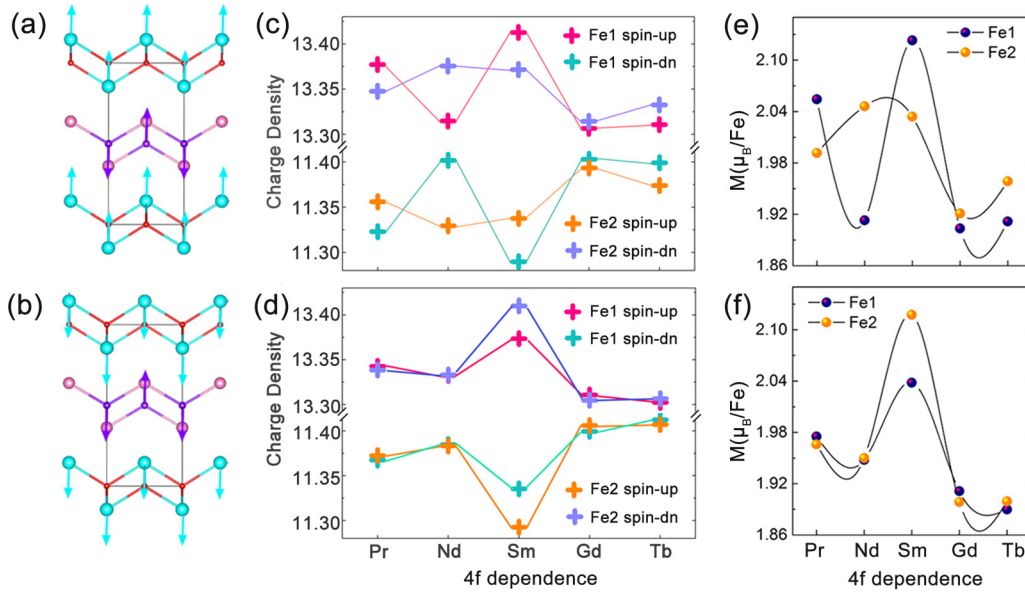


FIG. 5. (a) The magnetic order schematics of REFeAsO with the magnetic order of RE were set ferromagnetically coupled to Fe1. (b) The magnetic order of RE were set ferromagnetically coupled Fe2. (c, d) The charge density of Fe1 and Fe2 at the different magnetic directions of RE along Pr, Nd, Sm, Gd, and Tb. (e, f) The magnetic moments of Fe1 and Fe2 at the different magnetic directions of RE along Pr, Nd, Sm, Gd, and Tb.

4*f*-electron superconductive systems notably entangles the multipole degrees of freedom, which is a kind of so-called high-rank multipole [27]. The 4*f*-electron-containing 1111-type iron-superconductors might exhibit a spin reorientation from the *a-b* plane to *a-c* plane owing to the aforementioned coupling between RE and Fe, and thus it is reasonable to infer that the emergence of noncollinear magnetic order accompanies with high- T_c superconductivity. Therefore, we regard that the magnetic coupling from the rare earth elements should be taken into accounts when we investigate these 1111-type iron-superconductors. Finally, we find that among the selected rare earth elements, SmFeAsO presents the most obvious variation on both charge density and magnetic moments, and this is in good agreement with the fact that SmFeAsO_{1- δ} possesses the highest transition temperature [16].

Herein, taking SmFeAsO as an example, we get insight into the effect of 4*f* electrons on the Fermi surface. For this purpose, we carried out calculations on the electronic structures and Fermi surface by taking both electron correlation and spin-orbit coupling into accounts on Sm. For comparison, we also carried out similar calculations by the substitution of Sm by La. As shown in Figs. 6(a) and 6(b), the band crossing the Fermi level is mainly composed of Fe 3*d* orbitals and *f*-orbitals. Partial density of state analysis of *f* orbitals indicates that fz^3 orbital make the main contribution to the Fermi level [see Fig. 6(c)]. From this point of view, the distance between RE-O layers to the Fe-As block is a key structural parameter besides that it facilitates the charge transfer from RE-O to Fe-As block when electron/hole is doped. The comparison of the differential Fermi surface between without and with 4*f* contributions shown in Figs. 6(d) and 6(e) reveals that 4*f* electrons make much contribution to the Fermi surface. The 4*f* electrons contributing to the superconductivity was firstly discovered in the heavy-fermion material CeCu₂Si₂ in 1979 by F. Steglich *et al.* [52]. The specific-heat coefficient

$C/T \sim 0.75 \text{ J/mol} \cdot \text{CeK}^2$ at $T_c \sim 0.5 \text{ K}$ indicated that the heavy-fermion state had been formed by the strong electron correlation between *f* electrons. Heavy-fermion superconductors are prime candidates for novel electron-pairing states due to the spin-orbital degrees of freedom and electron correlations. Based on these statements and combining the above multiorbital degrees of freedom, we argue that the presence of strong spin-orbit coupling in the 4*f*-electron entangles these degrees of freedom, which leads to the so-called multipole degrees of freedom. Exotic electronic states resulting from entangled spin and orbital degrees of freedom are hallmarks of strongly correlated *f*-electron systems. We consider that the behavior of 4*f* electrons within these 1111-type iron-based superconductors is similar to that within heavy-fermion.

Within this paper, we concentrate our attention to the microscopic structural distortion effects in REFeAsO tuned by lanthanide contraction or external strain and rare-earth 4*f* electrons on iron-based superconductivity, which our theoretical results track well on the tendency discovered by previous experimental studies [14,16]. Based on the discussions herein, the natural connections between the unconventional superconductivity and synergistic effects: local structural distortions and 4*f* electrons, have been established in this theoretical study. Generally, it is clear that the calculations of this static mean field method with DFT + *U* and spin-orbital coupling are not good enough to describe strongly correlated systems, especially in *f*-electron-containing iron-based superconductors. Using the combination of density functional theory and dynamical mean field theory (DFT + DMFT), Yin *et al.* calculated a large number of iron-based superconductors in both their magnetic and paramagnetic states, which explained the strongly Fermi surface dependence on superconducting gaps observed in experiments [53]. Within the tight-binding model within first-principles calculations, Takuya Nomoto and Hiroaki Ikeda clarified the microscopic

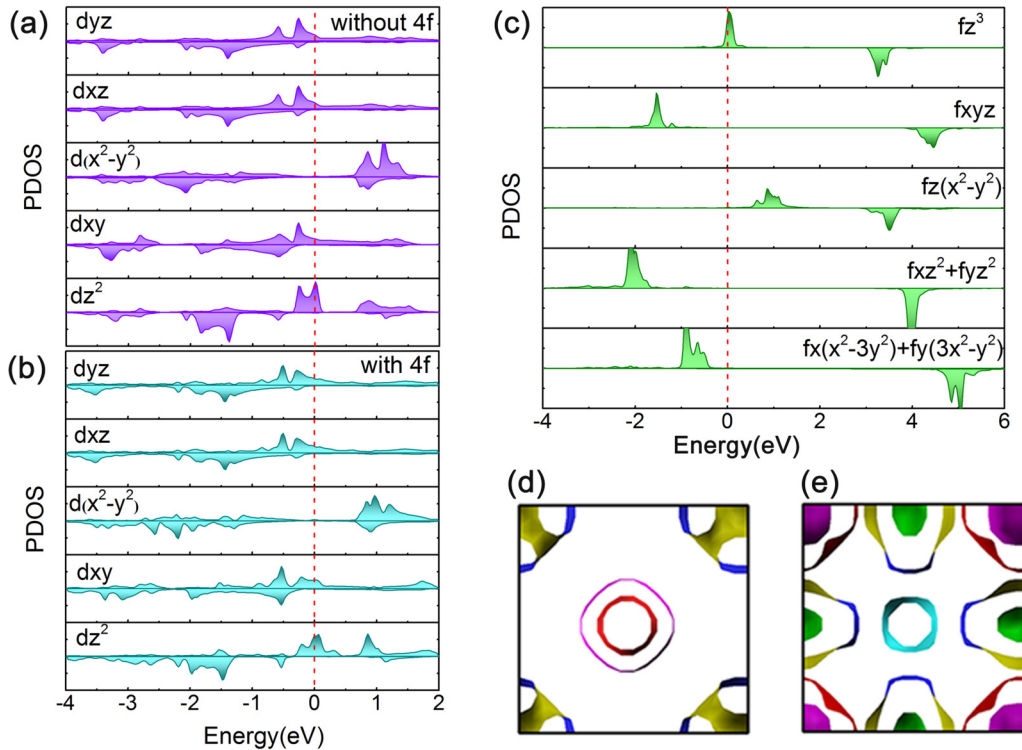


FIG. 6. (a) Fe2-3d partial DOS in SmFeAsO obtained without the effect of 4f electrons and (b) Fe2-3d partial DOS in SmFeAsO obtained with the effect of 4f electrons. (c) DOS of Sm 4f orbitals in SmFeAsO obtained at GGA + U + SOC level. (d) Fermi-surface of SmFeAsO without 4f electrons. (e) Fermi-surface of SmFeAsO taking account of the 4f electrons.

gap structure in the heavy-fermion superconductor UPt_3 [26]. Our present results might cause more researchers' attention on the issue of rare-earths particularity in the iron-based superconductors, and more advanced methods, such as those taking nonlinear magnetic coupling and dynamic effects into accounts, are anticipated. Therefore, further work is required to disentangle the tanglesome factors for superconductive mechanism both on advanced theoretical detections and decisive experimental evidence.

IV. CONCLUSIONS

In summary, we revisit 1111-type iron-based superconductors REFeAsO in which RE are La, Ce, Pr, Nd, Pm, Sm, Gd, Tb, Dy, Ho, Er, Tm, and Lu via first-principles calculations based on DFT methods. The mechanism of the high-temperature superconductivity is studied by taking both lanthanide contraction and external strain as fine structural distortion controllers. It is found that the rare earth elements on one hand modulate the microscopic structures so as to maximize the orbital degeneracy on the Fermi level, and

on the other hand their 4f electrons directly contribute to the superconductivity. Our findings reveal not only the long-standing puzzle in this iron-based material, but also urge us to reconsider the relationships between the superconductivity and rare earth elements in A sites. For iron-based superconductors, they provide us another interesting perspective to search for the mechanism of superconductivity since the orbital degrees of freedom are important ingredients in these materials. Clearly, the question of sophisticated mechanism in unconventional superconductivity is far from being resolved and further effort is needed from both experimental and theoretical communities.

ACKNOWLEDGMENTS

This work is supported by the National Natural Science Foundation of China under Grants No. 21571174, No. 51372244, and No. 21521092, Major Program of National Natural Science Foundation of China under Grant No. 21590794, and Special Program for Applied Research on Super Computation of the NSFC-Guangdong Joint Fund (the second phase).

-
- [1] Yoichi Kamihara, Takumi Watanabe, Masahiro Hirano, and H. Hosono, *J. Am. Chem. Soc.* **130**, 3296 (2008).
 [2] M. Rotter, M. Tegel, and D. Johrendt, *Phys. Rev. Lett.* **101**, 107006 (2008).
 [3] X. C. Wang, Q. Q. Liu, Y. X. Lv, W. B. Gao, L. X. Yang, R. C. Yu, F. Y. Li, and C. Q. Jin, *Solid State Commun.* **148**, 538 (2008).
 [4] X. Zhu, F. Han, G. Mu, P. Cheng, B. Shen, B. Zeng, and H.-H. Wen, *Phys. Rev. B* **79**, 220512 (2009).
 [5] I. I. Mazin, D. J. Singh, M. D. Johannes, and M. H. Du, *Phys. Rev. Lett.* **101**, 057003 (2008).
 [6] K. Kuroki, S. Onari, R. Arita, H. Usui, Y. Tanaka, H. Kontani, and H. Aoki, *Phys. Rev. Lett.* **101**, 087004 (2008).
 [7] F. Ma and Z.-Y. Lu, *Phys. Rev. B* **78**, 033111 (2008).

- [8] D. J. Singh and M. H. Du, *Phys. Rev. Lett.* **100**, 237003 (2008).
- [9] H. Usui, K. Suzuki, K. Kuroki, N. Takeshita, P. M. Shirage, H. Eisaki, and A. Iyo, *Phys. Rev. B* **87**, 174528 (2013).
- [10] L. Ortenzi *et al.*, *Phys. Rev. Lett.* **114**, 047001 (2015).
- [11] J. Zhao *et al.*, *Nat. Mater.* **7**, 953 (2008).
- [12] X. H. Chen, T. Wu, G. Wu, R. H. Liu, H. Chen, and D. F. Fang, *Nature* **453**, 761 (2008).
- [13] G. F. Chen, Z. Li, D. Wu, G. Li, W. Z. Hu, J. Dong, P. Zheng, J. L. Luo, and N. L. Wang, *Phys. Rev. Lett.* **100**, 247002 (2008).
- [14] Z. A. Ren, J. Yang, W. Lu, W. Yi, G. C. Che, X. L. Dong, L. L. Sun, and Z. X. Zhao, *Mater. Res. Innov.* **12**, 105 (2008).
- [15] K. Matano, Z. A. Ren, X. L. Dong, L. L. Sun, Z. X. Zhao, and G.-Q. Zheng, *Europhys. Lett.* **83** (2008).
- [16] Z.-A. Ren and Z.-X. Zhao, *Adv. Mater.* **21**, 4584 (2009).
- [17] M. R. Norman, *Science* **332**, 196 (2011).
- [18] J. Dong *et al.*, *Europhys. Lett.* **83**, 27006 (2008).
- [19] Q. Liu *et al.*, *J. Am. Chem. Soc.* **133**, 7892 (2011).
- [20] S. A. J. Kimber *et al.*, *Nat. Mater.* **8**, 471 (2009).
- [21] V. I. Anisimov and O. Gunnarsson, *Phys. Rev. B* **43**, 7570 (1991).
- [22] F. Wang and D.-H. Lee, *Science* **332**, 200 (2011).
- [23] Igor I. Mazin, *Nature* **464**, 183 (2010).
- [24] H. Ikeda, M.-T. Suzuki, R. Arita, T. Takimoto, T. Shibauchi, and Y. Matsuda, *Nat. Phys.* **8**, 528 (2012).
- [25] M. P. Smylie, H. Claus, U. Welp, W. K. Kwok, Y. Qiu, Y. S. Hor, and A. Snezhko, *Phys. Rev. B* **94**, 180510 (2016).
- [26] T. Nomoto and H. Ikeda, *Phys. Rev. Lett.* **117**, 217002 (2016).
- [27] H. Ikeda, M.-T. Suzuki, and R. Arita, *Phys. Rev. Lett.* **114**, 147003 (2015).
- [28] G. Kresse and J. Hafner, *Phys. Rev. B* **48**, 13115 (1993).
- [29] G. Kresse and J. Furthmuller, *Phys. Rev. B* **54**, 11169 (1996).
- [30] J. P. Perdew, K. Burke, and M. Ernzerhof, *Phys. Rev. Lett.* **77**, 3865 (1996).
- [31] J. P. Perdew and Y. Wang, *Phys. Rev. B* **33**, 8800 (1986).
- [32] X. J. Kong, C. T. Chan, K. M. Ho, and Y. Y. Ye, *Phys. Rev. B* **42**, 9357 (1990).
- [33] D. J. Singh and L. Nordström, *Planewaves, Pseudopotentials, and the LAPW Method* (Springer, Berlin, 2006).
- [34] K. Schwarz, P. Blaha, and G. K. H. Madsen, *Comput. Phys. Commun.* **147**, 71 (2002).
- [35] H. J. Monkhorst and J. D. Pack, *Phys. Rev. B* **13**, 5188 (1976).
- [36] V. I. Anisimov, J. Zaanen, and O. K. Andersen, *Phys. Rev. B* **44**, 943 (1991).
- [37] S. V. Borisenko *et al.*, *Nat. Phys.* **12**, 311 (2016).
- [38] Y. Chen, B. G. Ueland, J. W. Lynn, G. L. Bychkov, S. N. Barilo, and Y. M. Mukovskii, *Phys. Rev. B* **78**, 212301 (2008).
- [39] D. H. Lu *et al.*, *Nature* **455**, 81 (2008).
- [40] C. de la Cruz *et al.*, *Nature* **453**, 899 (2008).
- [41] S. Margadonna, Y. Takabayashi, M. T. McDonald, M. Brunelli, G. Wu, R. H. Liu, X. H. Chen, and K. Prassides, *Phys. Rev. B* **79**, 014503 (2009).
- [42] C. A. McElroy, J. J. Hamlin, B. D. White, S. T. Weir, Y. K. Vohra, and M. B. Maple, *Phys. Rev. B* **90**, 125134 (2014).
- [43] G. Xu, W. Ming, Y. Yao, X. Dai, S. C. Zhang, and Z. Fang, *Europhys. Lett.* **82**, 67002 (2008).
- [44] K. Haule, J. H. Shim, and G. Kotliar, *Phys. Rev. Lett.* **100**, 226402 (2008).
- [45] W. S. Kyung *et al.*, *Nat. Mater.* **15**, 1233 (2016).
- [46] C. Putzke *et al.*, *Sci. Adv.* **2**, e1501657 (2016).
- [47] S. A. J. Kimber *et al.*, *Phys. Rev. B* **78**, 140503 (2008).
- [48] J. Zhao *et al.*, *Phys. Rev. B* **78**, 132504 (2008).
- [49] T. Yildirim, *Phys. Rev. Lett.* **101**, 057010 (2008).
- [50] Q. Si and E. Abrahams, *Phys. Rev. Lett.* **101**, 076401 (2008).
- [51] Y. Shen, C. W. Li, X. Tang, H. L. Smith, and B. Fultz, *Phys. Rev. B* **93**, 214303 (2016).
- [52] F. Steglich, J. Aarts, C. D. Bredl, W. Lieke, D. Meschede, W. Franz, and H. Schafer, *Phys. Rev. Lett.* **43**, 1892 (1979).
- [53] Z. P. Yin, K. Haule, and G. Kotliar, *Nat. Mater.* **10**, 932 (2011).